Nonlinear Analysis: Real World Applications 13 (2012) 2459–2465

Contents lists available at SciVerse ScienceDirect

Nonlinear Analysis: Real World Applications

journal homepage: www.elsevier.com/locate/nonrwa

Emulating complex business cycles by using an electronic analogue

S. Bouali [a], A. Buscarino [b,c], L. Fortuna [b,c], M. Frasca [b,c,*], L.V. Gambuzza [b]

[a] Management Institute, Department of Economics, University of Tunis, Tunis, Tunisia

[b] Dipartimento di Ingegneria Elettrica Elettronica e Informatica, Università degli Studi di Catania, Viale A. Doria, 6 - 95125 Catania, Italy

[c] Laboratorio sui Sistemi Complessi, Scuola Superiore di Catania, Università degli Studi di Catania, Via Valdisavoia 9, 95123 Catania, Italy

ARTICLE INFO

Article history:
Received 9 December 2011
Accepted 19 February 2012

Keywords:
Nonlinear circuits
Economic cycles
Chaos
Bifurcations

ABSTRACT

Long run growth of the US national economic system, for example, reveals a strong oscillatory behavior due to complex interactions of aggregates. However, modelizations of such dynamics often assume that instability is the outcome of linear and additive cycles determined by exogenous shocks. In this work, a modelization of endogenous nonlinear and inseparable cycles is retained to explain the highly complex business cycle phenomenon. Bouali's system is built to this scope. Its numerical simulations exhibit a rich repertoire of nonlinear dynamical phenomena, but this paper introduces its electronic implementation. The robust plug and play chaotic circuit is designed to be easily realized using standard components in a rigorous, fast and inexpensive way. We find that experimental results display periodicity, bifurcations and chaos that match with high accuracy the corresponding theoretical values.

1. Introduction

From the early years of the 20th century, empirical studies of the National Bureau of Economic Research [1] have confirmed that economic aggregates (GDP, consumption, investment, . . .) follow expansion and contraction series. Such oscillatory motion embeds a vast spectrum of cycles [2] called seasonal cycles (within a year), Kitchin cycles (3 years), Juglar cycles (9–10 years), Kuznets cycles (15–20 years) and Kondratiev cycles (48–60 years). Obviously, every cycle exhibits a complete "four-phase" sequence (boom, recession, depression, recovery). However, theoretical modelization often assumed that oscillations are the outcome of "external" shocks (technological innovations, consumption jumps, natural catastrophes, . . .) distorting the steady state of the long run growth. Goodwin [3] introduced the idea that economic fluctuations result from endogenous interactions of the economic system itself and are not driven by exogenous shocks as assumed previously in academic literature.

In his seminal paper, Goodwin modelizes economic growth oscillation as the outcome of a struggle between the employment factor and capital according to the 2D Lotka–Volterra equations (LVE) [4,5]. However, LVE displays a unique cycle, in contrast to the real complex economic system running. Indeed, long run growth is fundamentally unpredictable since it is derived from deep and intricate economic interactions. LVE as a 2D model cannot display a wide spectrum of oscillations with different amplitudes and frequencies. To the scope of the extension of the oscillatory dynamics, the forcing of the 2D dynamical models could inject a new kind of instability to look like the data series of the economic aggregates. In this way, the modification of the 2D Van der Pol oscillator [6] with a feedback loop leads to a full 3D model with a rich repertoire of oscillations [7]. From the Van der Pol oscillator, complexity emerges by an endogenous linkage.

* Corresponding author at: Dipartimento di Ingegneria Elettrica Elettronica e Informatica, Università degli Studi di Catania, Viale A. Doria, 6 - 95125 Catania, Italy.

E-mail addresses: Safieddine.Bouali@isg.rnu.tn (S. Bouali), mfrasca@diees.unict.it (M. Frasca).

1468-1218/$ – see front matter © 2012 Elsevier Ltd. All rights reserved.
doi:10.1016/j.nonrwa.2012.02.010

This methodology is the "bridge" to generating complexity and constitutes the trigger mechanism of new dynamical patterns from basic 2D models. Small perturbations imply now large effects appearing in unpredictable and singular oscillations and chaotic ones. The hardware implementation of similar mathematical models constitutes the expected step following the classical computer simulations. Indeed, to display the wide range of dynamical patterns and the fascinating motion of chaos and its apparently erratic behavior, the physical processors developed are not only electronic chips but also mechanical machineries. For instance, the Lorenz model has been implemented in a specially engineered waterwheel developed at M.I.T. in the earlier 70's [8–10]. The design of such chaotic analogues emerged as fully experimental research accompanying the theoretical study of chaos [11,12]. Electronic circuits provide a systematic way to design and implement such analogues that can be then used for experimental characterization of the modeled dynamics [13].

This paper presents an in-depth study of a novel electronic circuit based on the chaotic model introduced in [7] that exhibits a wide spectrum of nonlinear dynamics. Its technical configuration has been chosen to achieve robustness, accuracy and ease-of-implementation criteria according to theoretical and experimental constraints. In particular, to design it the state variable approach discussed in [14] has been used.

The paper is organized as follows: in Section 2 the mathematical model considered is introduced, giving some insight into its relevance in economical modeling; Section 3 outlines the design procedure which leads to the implementation of the analogue electronic circuit of the chaotic model, while in Section 4 the experimental characterization of the implemented circuit is discussed; finally Section 5 gives some concluding remarks.

2. Bouali's equations

The chaotic system originally introduced by Bouali is suitable for use in emulating the behavioral complexity of the economic aggregates linked to the long run growth when adequate parameters of the state variables are chosen. It is derived from the phenomenon of capital flight observed in less developed countries [15], injecting disequilibrium in the capital market, perturbing several other economic aggregates. The state variables of this economic model are the savings (households) S, the gross domestic product Y, and the foreign capital inflow (net) F.

The savings dynamics is characterized by the following equation:

$$\frac{dS}{dt} = aY + p(Y^* - Y^2)S \tag{1}$$

where Y^* is the value of the potential gross domestic product, a is the variation of the marginal propensity to saving, and p is the fraction of capitalized profit.

The second dynamical equation that has to be considered refers to the gross domestic product:

$$\frac{dY}{dt} = \frac{-S + F}{v} \tag{2}$$

where v represents the capital–output ratio.

Finally, the dynamical equation of foreign financing is taken into account:

$$\frac{dF}{dt} = mS - rY \tag{3}$$

where m is the capital inflow–saving ratio, and r the debt refund–output ratio.

Hence, the bridge to finding the complete model is provided by a feedback loop connected to the two equations of the Van der Pol oscillator. The model overlaps with the 2D oscillator. It can be written by means of the following three rescaled coupled ordinary differential equations:

$$\begin{cases} \dot{x} = ky + \mu x(b - y^2) \\ \dot{y} = -x + sz \\ \dot{z} = px - qy \end{cases} \tag{4}$$

where k, μ, b, s, p, and q are positive parameters, and x, y, and z are dimensionless variables representative of savings, gross domestic product, and foreign capital inflow.

The model includes one nonlinearity in its first equation and displays three unstable equilibria: $E0$, which is the origin as the trivial solution, and $E1 = (\alpha, p/q\alpha, 1/s\alpha)$ and $E2 = (-\alpha, -(p/q)\alpha, -(1/s)\alpha)$, two antisymmetric points with $\alpha = [\mu b + k(p/q)]/[(p/q)^2\mu]^{1/2}$.

System (4) is able to reproduce a large repertoire of dynamical behaviors including limit cycles of different periods, chaos, and blue sky bifurcations. In particular, chaotic behavior can be obtained for a quite large range of parameters. We report two examples of chaotic behaviors, obtained for two different values of the bifurcation parameter s. The first example refers to the following set of parameters: $k = 0.02$, $\mu = 0.4$, $b = 0.2$, $p = 10$, $q = 0.1$, and $s = 50$. Fig. 1 shows the projection of this attractor in the phase planes x–z and y–z. The second example refers to the following set of parameters: $k = 0.02$, $\mu = 0.4$, $b = 0.2$, $p = 10$, $q = 0.1$, and $s = 110$. Fig. 2 shows the projection of this attractor in the phase planes

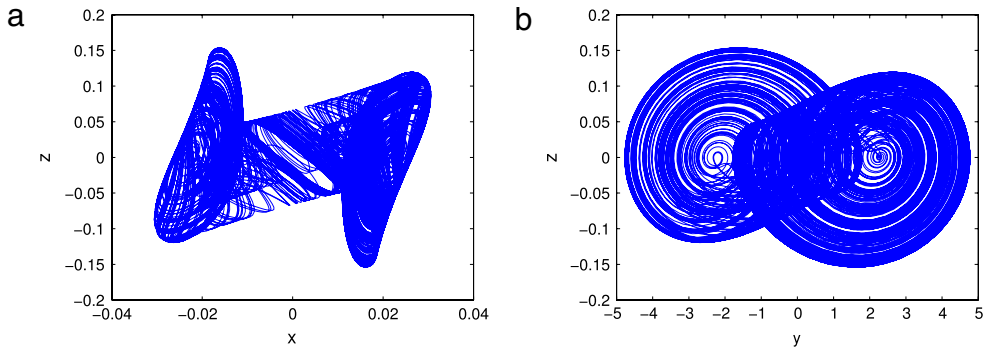

Fig. 1. Projections of the attractor for $s = 50$, double scroll: (a) x–z phase plane, (b) y–z phase plane.

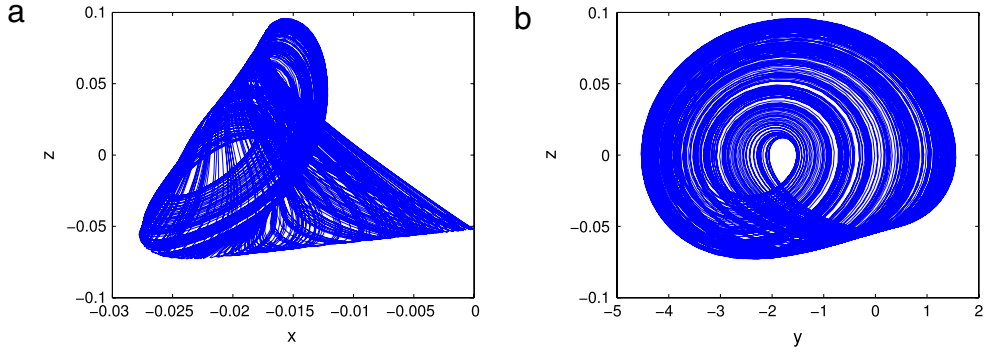

Fig. 2. Projections of the attractor for $s = 110$, single scroll: (a) x–z phase plane, (b) y–z phase plane.

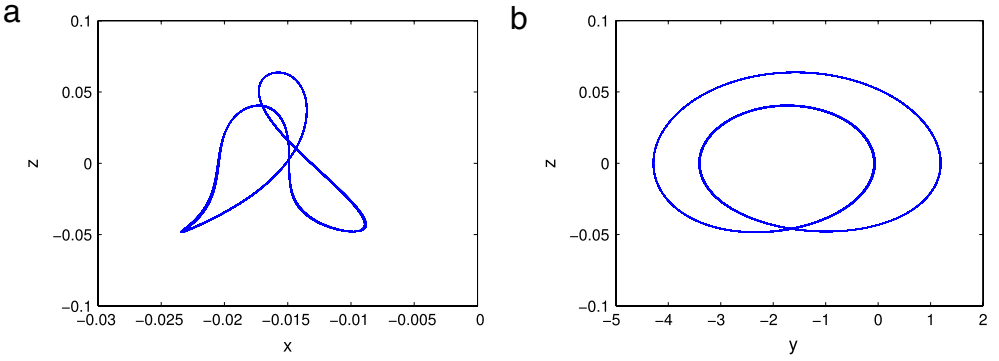

Fig. 3. Projections of the limit cycle for $s = 250$: (a) x–z phase plane, (b) y–z phase plane.

x–z and y–z. A further increase in the parameter s leads to the occurrence of periodic limit cycles, such as the one obtained for $s = 250$ and reported in Fig. 3.

In the next section, the physical implementation of system (4) is introduced. The first step in the design of this implementation is a suitable scaling of the dynamics of the mathematical model in order to match the physical constraints of the electronics used. After discussing this rescaled dynamics, the circuit will be presented and the experimental results reported.

3. Design of the circuit

Since the seminal work of Edward Lorenz [16] in 1963, chaos has rapidly become a fundamental subject of wide interest in many research fields and many efforts have been devoted to discovering new mathematical systems showing chaotic attractors. Chaos appears in a lot of different phenomena and soon chaotic phenomena came to fascinate circuit designers. The first chaotic circuit is the well-known Chua circuit [17] and it is remarkable that this circuit generating chaos is constituted of a very limited number of components (namely two capacitors, an inductor, a resistor and a Chua diode).

Following the Chua circuit, many other chaotic circuits have been designed. Some of them implement the dynamics of the mathematical systems showing chaos; others exploit the fundamental feature of electronic devices to show chaotic behavior. Examples of chaotic circuits exploiting the specific features of some electronic components are the Chua circuit [17] using a nonlinear component with piecewise linear characteristic, the circuits reported in [18–20] based on hysteretic elements and the circuits based on memristors discussed in [21–24], while switching devices interrupting the current in a coil or short-circuiting the voltage of a capacitor [25] and "disturbance of integration" [26] are other common mechanisms used in designing chaos generators.

The circuit implementing Bouali's equations has been designed by using a state variable approach, in which each state variable, i.e. x, y, z, is associated with the voltage across a capacitor, $C1, C2, C3$ respectively, and each dynamical equation is implemented through an operational amplifier (op-amp) in integrator configuration [14]. This approach requires that specific constraints on the amplitudes of state variables are satisfied. In fact, the oscillations have to be small enough to satisfy the limits imposed by power supply (otherwise they will saturate), and at the same time they have to be large enough to overcome the noise always present in electronic circuits.

In the case of Bouali's equations, the three dimensionless state variables x, y, z oscillate in the ranges $[-0.03; 0.03]$, $[-5; 5]$, $[-0.2; 0.2]$, respectively. In particular, the state variables x and z, having small amplitude (which can be comparable to the noise), need to be scaled up to oscillate in a larger range. Therefore, the rescaled system reads as

$$\begin{cases} \dot{X} = K\left[150kY + \mu X(b - 9Y^2)\right] \\ \dot{Y} = K\left[-\dfrac{1}{150}X + \dfrac{s}{12}Z\right] \\ \dot{Z} = K\left[\dfrac{4}{50}pX - 12qY\right] \end{cases} \tag{5}$$

where $X = 50x$, $Y = \frac{y}{3}$, $Z = 4z$, and $K = 3 \cdot 10^4$ is a time scaling factor which allows to reduce the observation time in experiments.

The circuit implementing system (5) is reported in Fig. 4. It is governed by the following equations:

$$\begin{aligned} \dot{X} &= k_1\left(-X + \frac{R_5}{R_1}X + \frac{R_5}{R_3}Y - \frac{R_5}{R_4}XY^2\right) \\ \dot{Y} &= k_2\left(-Y - \frac{R_{12}}{R_{10}}X + \frac{R_{12}}{R_7}Y + \frac{R_{12}}{R_9}Z\right) \\ \dot{Z} &= k_3\left(-Z + \frac{R_{18}}{R_{16}}X - \frac{R_{18}}{R_{17}}Y + \frac{R_{18}}{R_{15}}Z\right) \end{aligned} \tag{6}$$

where $k_1 = \frac{1}{R_6C_1}$, $k_2 = \frac{1}{R_{13}C_2}$, $k_3 = \frac{1}{R_{19}C_3}$.

The circuit makes use of two *AD*633 multipliers implementing the nonlinearity of the system, with the following input–output characteristics:

$$W = \frac{(I_1 - I_2)(I_3 - I_4)}{10V} + Z. \tag{7}$$

Components of the circuit have been chosen in order to match Eq. (5). In particular, parameter values can be fixed according to the following relations:

$$\begin{aligned} k &= \frac{10}{3}\frac{R_5}{150R_3} \\ \mu &= \frac{10}{3}\frac{R_5}{9R_4} \\ \mu b &= \frac{10}{3}\left(\frac{R_5}{R_1} - 1\right) \\ p &= \frac{50}{4}\frac{R_{18}}{R_{16}} \\ q &= \frac{R_{18}}{12R_{17}} \\ s &= \frac{22}{100}\left(1 + \frac{R_{21}}{R_{20}}\right)\frac{12R_{12}}{R_9}. \end{aligned} \tag{8}$$

The component values listed in the caption of Fig. 4 allow us to realize the parameter values reported in the previous section.

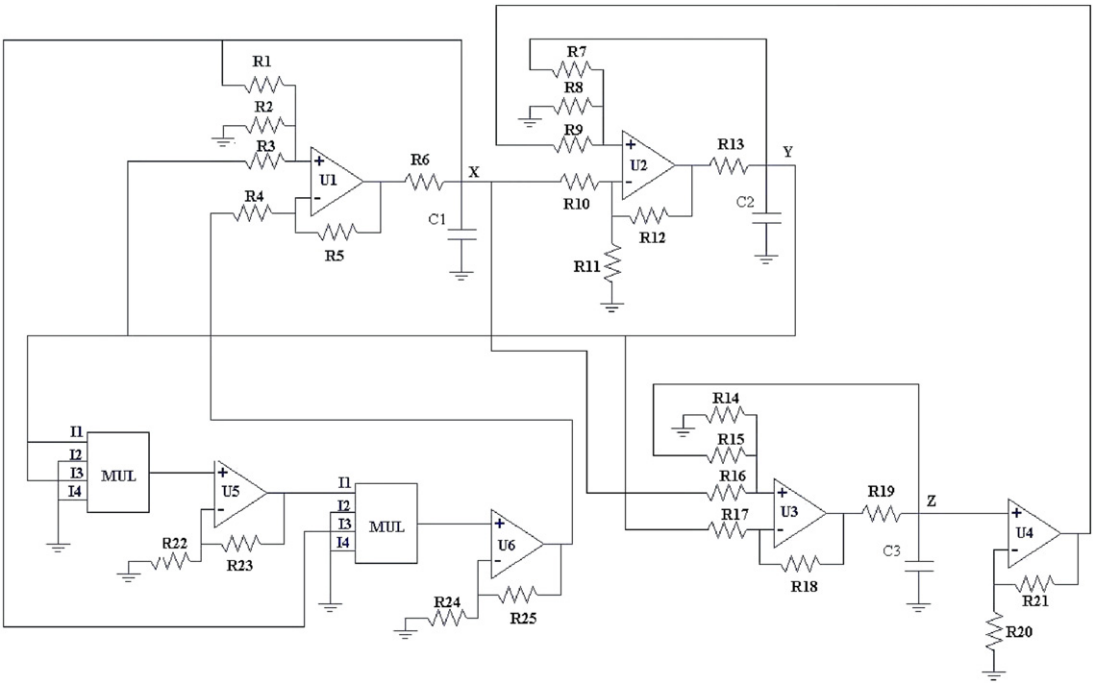

Fig. 4. Schematic of the circuit implementing Bouali's equations. The values of the components are the following: $R1 = 9.76\ \text{k}\Omega$, $R2 = 57.5\ \text{k}\Omega$, $R3 = 10\ \text{k}\Omega$, $R4 = 8.3\ \text{k}\Omega$, $R5 = 10\ \text{k}\Omega$, $R6 = 100\ \Omega$, $R7 = 10\ \text{k}\Omega$, $R8 = 700\ \Omega$, $R9 = 1.72\ \text{k}\Omega$, $R10 = 299\ \text{k}\Omega$, $R11 = 500\ \Omega$, $R12 = 10\ \text{k}\Omega$, $R13 = 1.5\ \text{k}\Omega$, $R14 = 242.3\ \text{k}\Omega$, $R15 = 100\ \text{k}\Omega$, $R16 = 127\ \text{k}\Omega$, $R17 = 83.3\ \text{k}\Omega$, $R18 = 100\ \text{k}\Omega$, $R19 = 300\ \Omega$, $R20 = 1\ \text{k}\Omega$, $R22 = 1\ \text{k}\Omega$, $R23 = 9\ \text{k}\Omega$, $R24 = 1\ \text{k}\Omega$, $R25 = 9\ \text{k}\Omega$, $C1 = C2 = C3 = 100nF$. $R21$, which implements the bifurcation parameter s, is a variable resistor. *TL*084 op-amps and *AD*633 multipliers have been used.

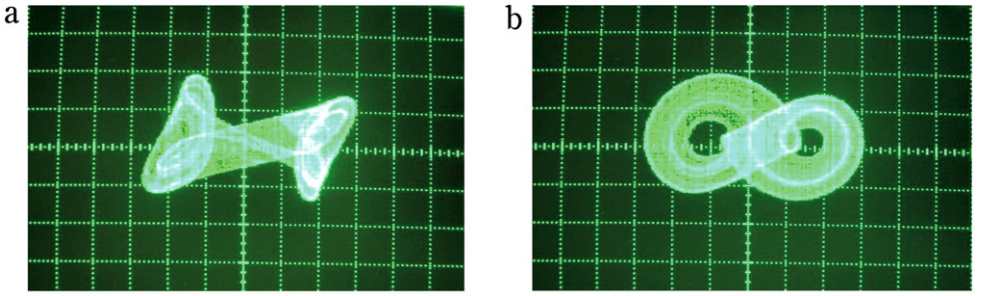

Fig. 5. Chaotic attractor exhibited by the circuit for $s = 50$: projections on the (a) X–Z and (b) Y–Z phase planes (horizontal axis: 500 mV/div; vertical axis: 500 mV/div).

4. Experimental results

The circuit has been implemented in our lab with off-the-shelf discrete components. The waveforms have been displayed on the oscilloscope for a first investigation of the circuit by visual inspection and then the corresponding data have been acquired by using a National Instruments (NI-USB6251) data acquisition board with a sampling frequency $f_s = 750$ kHz.

In order to investigate the behavior of the system with respect to s, the value of resistor R_{21} has been varied using a 20 kΩ trimmer, such that $s = s(R_{21})$ is changed in the system. The exact dependence of parameter s on R_{21} is given by Eqs. (8). The chaotic attractor shown by the circuit when $R_{21} = 2.3\ \text{k}\Omega$, corresponding to $s \approx 50$, is reported in Fig. 5. Comparing these projections with the numerical results shown in Fig. 1, a good agreement can be observed. Increasing the bifurcation parameter, the circuit shows the transition from a double-scroll to a single-scroll attractor. The behavior of the circuit with $R_{21} = 6\ \text{k}\Omega$, implementing $s \approx 110$, is reported in Fig. 6, which is similar to the numerical simulations reported in Fig. 2. Finally, for $R_{21} = 15.3\ \text{k}\Omega$ the behavior of the circuit is a periodic limit cycle, reported in Fig. 7, corresponding to an implemented value of $s \approx 250$, which can be compared to the model behavior reported in Fig. 3.

The behavior of the circuit has been characterized with respect to the bifurcation parameter s (see Fig. 8). The experimental bifurcation diagram, reported in Fig. 8, has been obtained by varying R_{21} in steps of 65 Ω corresponding to a unitary increasing of s. The relative maxima Y_{MAX} of the second state variable are reported for each value of the parameter s.

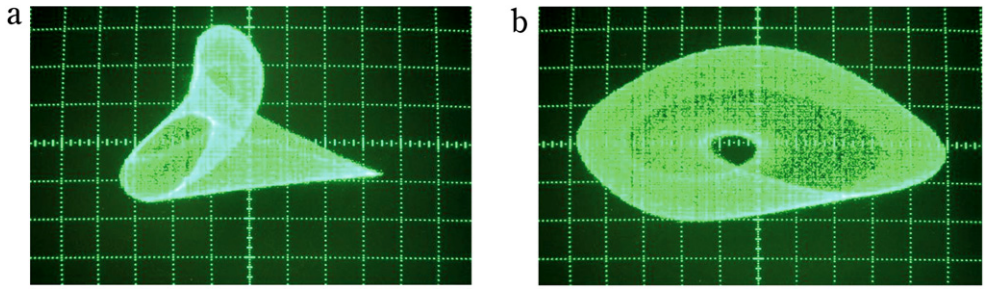

Fig. 6. Chaotic attractor exhibited by the circuit for $s = 110$: projections on the (a) X–Z (horizontal axis: 200 mV/div; vertical axis: 200 mV/div) and (b) Y–Z phase planes (horizontal axis: 100 mV/div; vertical axis: 200 mV/div).

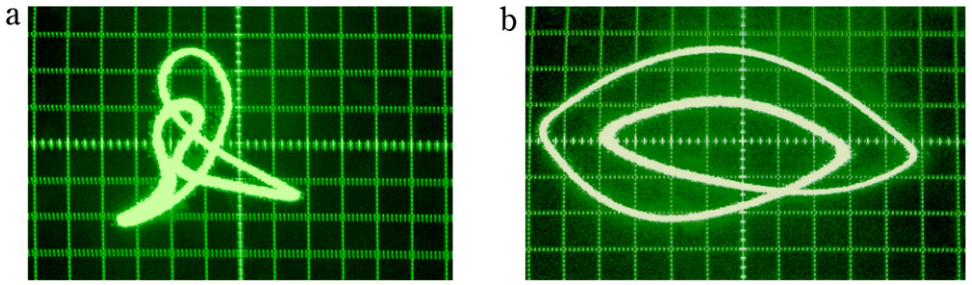

Fig. 7. Limit cycle exhibited by the circuit for $s = 250$: projections on the (a) X–Z (horizontal axis: 200 mV/div; vertical axis: 200 mV/div) and (b) Y–Z phase planes (horizontal axis: 100 mV/div; vertical axis: 200 mV/div).

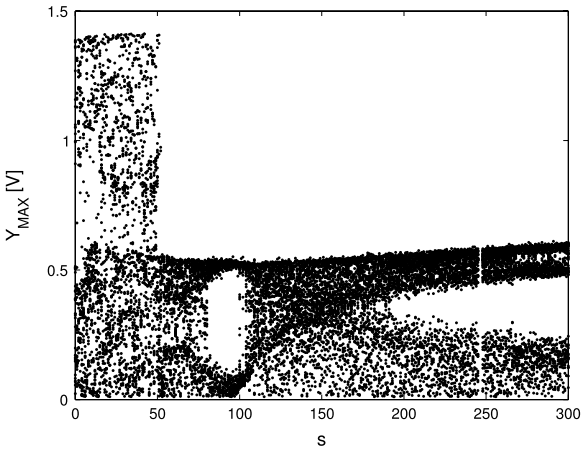

Fig. 8. Experimental bifurcation diagram with respect to $s = s(R_{21})$ (the exact dependence is given by Eqs. (8)) for the circuit implementing Bouali's equations.

The bifurcation diagram shows the chaotic regions of the system behavior, the periodic windows and the transition from a double-scroll to a single-scroll case occurring approximatively for $s \approx 50$. Around the crisis an intermittent behavior (bursting behavior) appears. This is shown in Fig. 9, showing the waveform exhibited by the circuit for $R_{21} = 2.6\ \text{k}\Omega$ which corresponds to $s \approx 52$. Therefore, around this critical value of the parameters, the dynamical model exhibits a breaking point simulating the classic signs of the economic bursts. The system does not collapse but displays an intermittent behavior. The economic system suddenly falls into a re-adjustment process diving the overvalued investments, for example, to a restricted range of oscillation. Financial market exuberance vanishes and the dynamical trend is driven to an utterly different path in a brutal way.

5. Concluding remarks

Modelization of the long-term economic trend should display the complex interaction of its major variables. Bouali's system as an elementary nonlinear dynamical model with a limited number of equations leads to a very wide range of behaviors. With a unique nonlinear equation, the system induces patterns similar to the data series of the real economy.

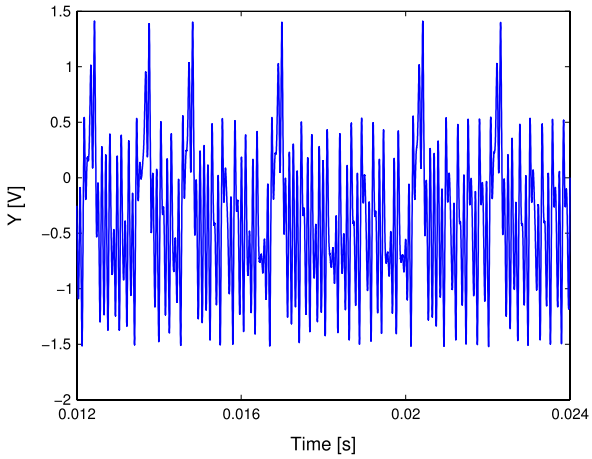

Fig. 9. Experimental waveform of the Y variable obtained for $R_{21} = 2.6$ kΩ which corresponds to $s \approx 52$. Around the crisis, bursting behavior appears.

This paper proposes a discrete component circuit implementation of this model alongside its computational simulations. The realization of physical processors obeying chaotic dynamical equations is fundamental for experimental research on chaos and nonlinear dynamics in general. By adopting an approach based on state variables, an electronic analogue emulating Bouali's equation and constituted of only common, low-cost circuital components, like resistors, capacitors, op-amps and analogue multipliers, has been presented. The experimental behavior tested and compared with the numerical simulations replicates the whole dynamical range exhibited by the corresponding theoretical model, thus validating the possibility of using the circuit introduced to experimentally study chaos in economic cycles. Measures confirm the correct physical implementation, high throughput, and robustness of the nonlinear circuit. While the present circuit as well as other chaotic circuits can also find applications as a random number generator [14] or in secure communications [27], it chiefly implements a model in accordance with the complex behavior of the long run growth of the contemporary globalized economy. Complexity of the real world implies complexity of its representation tools.

References

[1] National Bureau of Economic Research, 2011. Available online at: http://www.nber.org/cycles.html.
[2] J.A. Schumpeter, Business Cycles. A Theoretical, Historical and Statistical Analysis of the Capitalist Process, McGraw-Hill Book Company, New York, Toronto, London, 1939.
[3] R.M. Goodwin, A growth cycle, in: C.H. Feinstein (Ed.), Socialism, Capitalism and Economic Growth, Cambridge University Press, Cambridge, 1967.
[4] A.J. Lotka, Elements of Physical Biology, Williams & Wilkins Co., Baltimore, 1925
[5] V. Volterra, Variazioni e fluttuazioni del numero d'individui in specie animali conviventi, Mem. R. Accad. Naz. dei Lincei, Ser. VI 2 (1926).
[6] B. Van der Pol, On relaxation–oscillations, The London, Edinburgh and Dublin Phil. Mag. & J. Sci. 2 (7) (1927) 978–992.
[7] S. Bouali, Feedback loop in extended Van Der Pol's equation applied to an economic model of cycles, Internat. J. Bifur. Chaos 9 (1999) 745–756.
[8] E.N. Lorenz, The Essence of Chaos, University of Washington Press, Seattle, Washington, 1993.
[9] C. Sparrow, The Lorenz Equations: Bifurcations, Chaos, and Strange Attractors, Springer-Verlag, New York, 1982.
[10] L.E. Matson, The Malkus–Lorenz water wheel revisited, Amer. J. Phys. 75 (2007) 1114–1122.
[11] M. Kolà, G. Gumbs, Theory for the experimental observation of chaos in a rotating waterwheel, Phys. Rev. A 45 (1992) 626–637.
[12] Y. Liu, Q. Yang, Dynamics of a new Lorenz-like chaotic system, Nonlinear Anal. RWA 11 (2010) 2563–2572.
[13] X.-F. Li, K.E. Chlouverakis, D.-L. Xu, Nonlinear dynamics and circuit realization of a new chaotic flow: a variant of Lorenz, Chen and Lü, Nonlinear Anal. RWA 10 (2009) 2357–2368.
[14] L. Fortuna, M. Frasca, M.G. Xibilia, Chua's Circuit Implementations: Yesterday, Today and Tomorrow, World Scientific, 2009.
[15] J.T. Cuddington, Capital Flights: Estimates, Issues and Explanations, in: Princeton Studies in Int. Finance, vol. 58, 1986.
[16] E.N. Lorenz, Deterministic nonperiodic flow, J. Atmospheric Sci. 20 (1963) 130–141.
[17] R.N. Madan, Chua's Circuit: A Paradigm for Chaos, in: World Scientific Series on Nonlinear Sciences, Series B, vol. 1, World Scientific, Singapore, 1993.
[18] T. Saito, Reality of chaos in four-dimensional hysteretic circuits, IEEE Trans. Circuits Syst. I 38 (12) (1991) 1517–1524.
[19] K. Mitsubori, T. Saito, A four-dimensional plus hysteresis chaos generator, IEEE Trans. Circuits Syst. I 41 (12) (1994) 782–789.
[20] L. Fortuna, M. Frasca, S. Graziani, S. Reddiconto, A chaotic circuit with ferroelectric nonlinearity, Nonlinear Dynam. 44 (1–4) (2006) 55–61.
[21] M. Itoh, L.O. Chua, Memristor oscillators, Internat. J. Bifur. Chaos 18 (2008) 3183–3206.
[22] B. Muthuswamy, Implementing memristor based chaotic circuits, Internat. J. Bifur. Chaos 20 (2010) 1335–1350.
[23] B. Muthuswamy, Simplest chaotic circuit, Internat. J. Bifur. Chaos 20 (2010) 1567–1580.
[24] A. Buscarino, L. Fortuna, M. Frasca, L.V. Gambuzza, G. Sciuto, Memristive chaotic circuits based on cellular nonlinear networks, Internat. J. Bifur. Chaos 22 (3) (2012) 1250070-1-13.
[25] G. Chen, T. Ueta (Eds.), Chaos in Circuits and Systems, in: World Scientific Series on Nonlinear Science, Series B, vol. 11, 2002.
[26] E. Lindberg, K. Murali, A. Tamasevicius, The smallest transistor-based nonautonomous chaotic circuit, IEEE Trans. Circuits Syst. II 52 (10) (2005) 661–664.
[27] S. Hayes, C. Grebogi, E. Ott, Communicating with chaos, Phys. Rev. Lett. 70 (1993) 3031–3034.